SYSTEM BEHAVIOUR OF A MULTIPLE OVERCONSTRAINED COMPLIANT FOUR-BAR MECHANISM

Werner W.P.J. van de Sande, Ronald G.K.M. Aarts, and Dannis M. Brouwer
Mechanical Automation and Mechatronics
University of Twente
Enschede, the Netherlands

ABSTRACT

A method is proposed to identify the critical misalignment of a multiple overconstrained mechanism. This misalignment indicates the limit of desirable behaviour. The proposed method is compared with a multibody simulation of a compliant four-bar mechanism with three overconstraints. Subsequently, both analyses are compared to an experimental setup.

The proposed method compares well to the multibody model. The proposed method and multibody simulation match qualitatively with measurements of the four-bar mechanism. However, the measured critical misalignments are about 30% larger in the experiment. As such, the proposed method is able to compute the critical misalignment of the four-bar mechanism.

INTRODUCTION

Compliant mechanisms are used in precision mechanics to mitigate the effects of play, among others. In theory, their behaviour is predictable and deterministic. To obtain deterministic behaviour in an assembled mechanism, the principle of exact constraint design is often used.

Misalignments increase the internal stress in the mechanism. In an exactly constrained design the increase of internal stress due to misalignment is minimised. Yet these mechanisms can also suffer from limited load carrying capability and asymmetric and complex design. Overconstrained designs do not suffer from these drawbacks, but have a relatively small tolerance on misalignment. In a flexure-based mechanism this will cause unwanted static and dynamic system behaviour, such as buckling and change in support stiffness. The deterministic behaviour is therefore no longer guaranteed [1, 2].

The consequences of misalignment on a once-overconstrained parallel leaf spring guidance were investigated by Meijaard et al. [1]; a small misalignment in the overconstrained direction caused buckling and significant changes in the support stiffness and dynamic system behaviour.

This article aims to find a computationally inexpensive method to ascertain the limits of the deterministic behaviour of an overconstraint compliant mechanism by determining the critical misalignment. As such, the work outlined in this article can be used as a guideline to estimate the manufacturing and assembly tolerances of an overconstrained flexure-based mechanism.

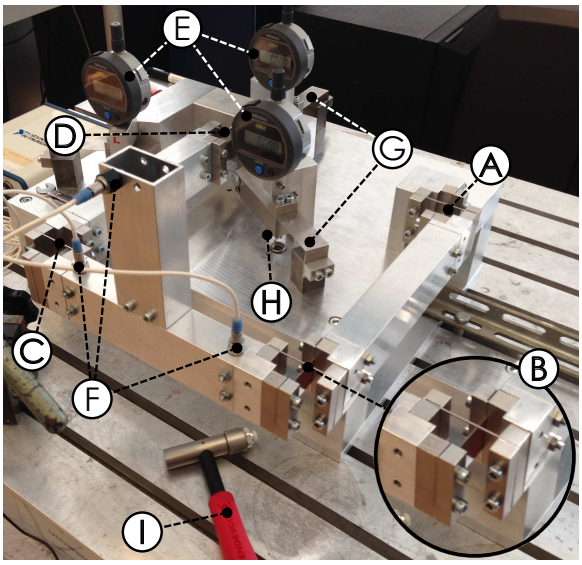

FIGURE 1. Photo of the experimental four-bar mechanism, with the cross pivot flexures (A,B,C,D) between the bars, dial gauges (E) on the manipulator and accelerometers (F) on the effector, 3 in-plane folded leaf spring constraint elements (G), 3 out-of-plane adjustment screws for the misalignment (H) and a modal hammer (I) to excite the mechanism.

SYSTEM DESCRIPTION

The four-bar mechanism under consideration is shown in figure 1. The four hinges are equal, both in dimension and orientation. A hinge is de-

signed to be exactly constrained; it has no overconstraints and one compliant rotation. A hinge consists of one leaf spring and two slender rods (inset B of figure 1); this cross pivot flexure is compliant for rotation along the vertical axis at the intersection of the leaf spring and the slender rods.

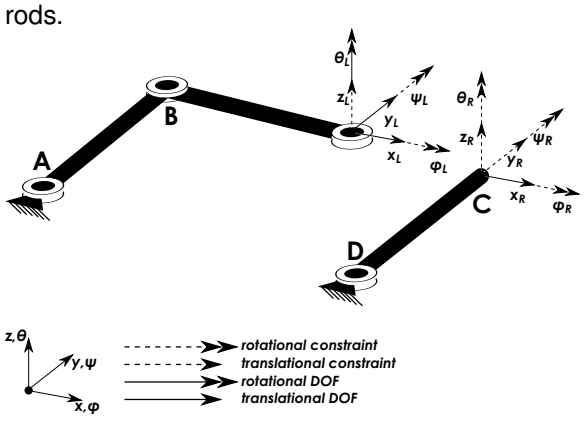

FIGURE 2. The kinematics of a four-bar mechanism illustrated by opening the loop at hinge C; the constraints of the left and right side are shown.

These flexures are used as hinges in conjunction with three rigid bars and the base to create the four-bar mechanism. The resulting mechanism has one degree of freedom (DOF) and three overconstraints. These can be illustrated by opening the mechanism at hinge C (figure 2). The in-plane directions of the mechanism are x, y and θ, whereas the out-of-plane directions are z, ϕ and ψ. Each hinge constrains five directions and leaves one free. The left side of the loop has three hinges and therefore has all in-plane DOFs. The right side of the loop has one in-plane DOF, the combined x_R and θ_R motion, since it only contains one hinge. This is the DOF of the mechanism. The three constraints from the left, z_L, ϕ_L and ψ_L, are equal to the constraints z_R, ϕ_R and ψ_R from the right side. Therefore the mechanism is three-times overconstrained [2].

The effects of these overconstraints can be shown by manipulating the three corresponding misalignments, the z- , ϕ- and ψ-misalignments, at one end of the mechanism; in this case it is the centre of compliance of hinge D. This manipulated point allows for independent control of each misalignment. The three independent misalignments can be controlled by three adjustment screws (H in figure 1). Gauges are used (E in figure 1) to measure the displacements. The specific misalignment at the manipulator (between D and G in figure 1) can be inferred from these displacements.

METHOD

A method is presented to provide insight into the possible effects of overconstraints as well as to simplify the problem of determining the buckling behaviour. The loop buckling analysis presented in this section divides the analysis of the buckling behaviour into two problems. First the forces in the mechanism due to a misalignment must be determined; second the buckling loads of the flexible elements of the mechanism are determined. The combination of these two parts leads to a relation between misalignment and the buckling behaviour of the flexures.

The relation between misalignment and stresses and forces in the mechanism is analysed. To that end, the equivalent compliance of the mechanism at the manipulator is determined. Several assumptions are made to calculate this equivalent compliance for this case. The four-bar mechanism is in its neutral position and will not deflect significantly if misalignment is added. Furthermore, the bars are considered infinitely stiff and the hinges are considered infinitesimally small. This allows for the computation of the equivalent stiffness of the mechanism as a serial loop of rigid bars and compliant hinges, which can deform in six directions.

Since the bars are rigid, the hinges are the only components in the mechanism that will be able to buckle. By means of free body diagrams the forces acting on each hinge are then determined from the forces acting on the mechanism at the manipulator. These resultant force vectors at the hinges are used in an analysis of the buckling behaviour of the hinges.

Due to the topology of the hinges, the compliance of the hinges can be lumped to the centre of compliance of the flexures. In this case this is at the intersection of the leaf spring and the slender rod flexure. The centre of compliance is the point in certain flexures where a force or moment in a certain direction will only cause a displacement in that same direction [3].

A finite element approach is used to determine the equivalent compliance. The hinges are treated as an infinitesimally small spring element

which can deform in all six directions. The bars of the mechanism are rigid. A set of nodal coordinates $x^{(k)}$ describe the locations and orientations of the nodes of an element k. Deformation coordinates $\epsilon^{(k)}$ are used to describe the deformation of an element. These are invariant for the rigid bars; for the hinges they describe the elastic deformation due to forces [2].

The compliance matrix is the same for every hinge. The force vector $\boldsymbol{f}^{(h)}$ is specific for a hinge. Expressions for all nodal coordinates are determined using the finite element approach. These expressions are functions of the forces in the mechanism. The same holds for the coordinates of the end node q of hinge D; this node is the manipulated point. The forces at the hinges are related to an input force vector at that node; the forces at hinges, $\boldsymbol{f}^{(A)}$, $\boldsymbol{f}^{(B)}$ and $\boldsymbol{f}^{(C)}$, are written as a function of the forces at hinge D, $\boldsymbol{f}^{(D)}$. Consequently, the resulting coordinate vector $\boldsymbol{x}_q^{(D)}$ is a function of the input force vector $\boldsymbol{f}^{(D)}$. The equivalent compliance of the mechanism at the coordinate $\boldsymbol{x}_q^{(D)}$ is the Jacobian matrix of that vector function. The change in the nodal coordinate vector $\boldsymbol{x}_q^{(D)}$ describes the added misalignment.

The three overconstraints in the mechanism lead to forces and moments on the hinges which can cause them to buckle. The buckling multiplier of a hinge is the ratio between the critical buckling load in a direction and the magnitude of the applied force vector in that same direction.

The equivalent stiffness at the manipulator is used to determine the explicit forces at the manipulator; these are related to specific amounts of misalignment. For each applied misalignment the resultant forces at the hinges are calculated. The three possible misalignments yield three explicit force vectors at the manipulator. There are four hinges in the mechanism; in total there will be twelve buckling cases.

Initially the resultant forces are used in a multibody simulation of a single hinge. The program SPACAR [4] can then determine the buckling multipliers and modes of the specific buckling case. The twelve unique buckling cases are all simulated.

The buckling loads were also estimated using the classical buckling equations [5].The resultant force vector can be factored into two components: the part responsible of the lateral buckling of the leaf spring and the part responsible of the axial buckling of one of the slender rods. The corresponding component of the resultant force vectors is compared to the estimated critical buckling loads in the same direction to determine the buckling multipliers.

A full elastic multibody simulation of the mechanism serves as a reference and is compared to the loop buckling analysis. Elastic beams are only used for the flexures of the hinges. Each hinge is modelled with twelve flexible beams; four for the leaf spring and four for each of the two slender rods. The torsional stiffness of the leaf spring is stiffened at the end to take into account constraint warping effects [6].

METHOD RESULTS

The results of the two methods are shown in table 1. The lowest critical misalignment of a hinge is listed in bold: at that specific misalignment at the manipulator that hinge will buckle. The difference between the methods is probably caused by an incorrect estimate of the effective lengths of the flexures. The equivalent length is hard to estimate; the buckling problem of the flexures has elastic constraints.

TABLE 1. The critical misalignments obtained with the simulation (sim) and the classical equations (eq) with respect to the hinges. The lowest misalignments are listed in bold.

hinge		A	B	C	D
$z(mm)$	eq	**2.15**	**2.15**	**2.15**	**2.15**
	sim	**2.33**	**2.33**	**2.33**	**2.33**
$\phi(mrad)$	eq	**11.5**	21.5	21.5	**11.5**
	sim	**11.9**	23.9	23.9	**11.9**
$\psi(mrad)$	eq	15.1	15.1	**6.28**	**6.28**
	sim	16.7	16.7	**6.99**	**6.99**

The mechanism simulation shows agreement with the hinge simulation with respect to the ϕ- and ψ-misalignments (table 2). The buckling mode is consistent with both the hinge simulation and the classical buckling equations. For instance, it can be seen in table 1 that hinges C and D buckle first due to a ψ-misalignment; the mechanism simulation also shows this behaviour.

TABLE 2. The calculated and simulated buckling misalignments of the mechanism

misalignment	$z(mm)$	$\phi(mrad)$	$\psi(mrad)$
mechanism sim	2.01	12.0	7.22
hinge sim	2.33	11.9	6.99
classical eq.	2.15	11.5	6.28

EXPERIMENT

The dynamic behaviour is measured with the help of a modal analysis. The vibrations of the effector are measured with three acceleration sensors; the mechanism is excited with a modal hammer. Frequency response functions are then determined using these four signals. Four vibration modes of the effector are measured. Of these four modes the third mode showed the most illustrative changes in the system behaviour. The third mode is the motion of the effector in the ψ-direction (figure 2). The misalignment was increased until visible buckling occurred. The results concerning the ψ-misalignment are shown in figure 3.

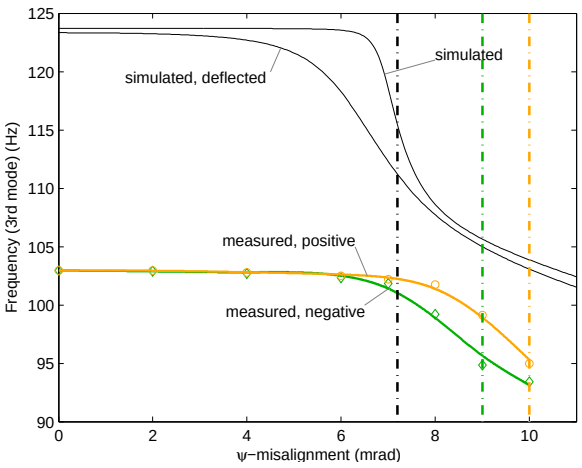

FIGURE 3. Modal profiles of the third mode due to a ψ-misalignment, with the simulated values in black (both negative and positive), the negative measured values in green and the positive measured values in orange. The critical misalignments are the dashed lines, again black for the value found in the simulation, green for the value at negative visible buckling and orange for the positive value.

The mechanism in the simulatation was deflected by half the thickness of the leaf spring flexures (250 μm) to simulate imperfections in the neutral position. A small deflection causes a significant change in the slope of the frequency change (figure 3). Qualitatively, the dynamic behaviour of the experiment matches with the simulation of the deflected mechanism. The buckling misalignment is higher, and therefore more tolerant, in the experimental setup. The average critical misalignment found in the experiment is about 2.5 $mrad$ larger than the simulated and calculated values: about 9.5 $mrad$. The hardware imperfections may influence the boundary conditions of the buckling problem of the slender rods. Still, the measured critical misalignment is only 30% higher than the calculated value, which is rather accurate considering the possible hardware imperfections. Also, this specific mechanism displayed only about a 10% decrease in stiffness in the ψ-direction at the critical misalignment.

The modal measurement on the experimental setup gave distinguishable results. The combination of spring steel flexures and steel clamping blocks resulted in a mechanism with a high Q factor.

CONCLUSION

The system behaviour of a multiple overconstrained compliant four-bar mechanism has been investigated. All approaches yielded values for the critical misalignment in the mechanism in the three overconstrained directions. Agreement was found between these approaches.The buckling misalignments could also be adequately estimated with classical methods. The critical misalignments found in the experiment were consistently higher than those found in the theoretical and numerical calculations: they were about 30% higher.

Importantly, the critical misalignments can be obtained without using complex simulations. The values obtained from the loop buckling analysis compare well with multibody simulations. These misalignments can be used to determine the manufacturing tolerances of a mechanism. The approach outlined in this article can be adapted to fit other types of compliant mechanisms.

REFERENCES

[1] J P Meijaard, D M Brouwer, J B Jonker. Analytical and experimental investigation of a parallel leaf spring guidance. Multibody system dynamics. 2010;23(1):77–97.

[2] D M Brouwer, S E Boer, J P Meijaard, R G K M Aarts. Optimization of release loca-

tions for small self-stress large stiffness flexure mechanisms. Mechanism and machine theory. 2013;64:230–250.

[3] H J M R Soemers. Design Principles for Precision Mechanisms. Enschede: T-Pointprint; 2010.

[4] J B Jonker, J P Meijaard. SPACAR — Computer Program for Dynamic Analysis of Flexible Spatial Mechanisms and Manipulators. In: Multibody Systems Handbook. Springer Berlin Heidelberg; 1990. p. 123–143.

[5] S P Timoshenko, J M Gere. Theory of Elastic Stability. 2nd ed. New York: McGraw-Hill; 1961.

[6] D H Wiersma, S E Boer, R G K M Aarts, D M Brouwer. Large stroke performance optimization of spatial flexure hinges. In: Proceedings of the IDECT ASME 2012. ASME; 2012. p. 1–10.